

Finally a similar field scale technique could serve to improve the detection of seismic precursors to landslides and earthquakes (Poli 2017). However, the application of ultrasonic waves in understanding the physical processes in granular materials and their potential in detecting seismic precursors has not been fully explored.

This study is inspired by this idea and aims at simulating the granular fill materials as a thin layer of Ottawa sand being sheared in a single direct shear apparatus. In order to reproduce similar stress conditions in the field and study the impact of normal stress reduction, the granular layers were first sheared up to the steady state condition, and then the normal stress was reduced gradually while the shear stress was kept constant. Active ultrasonic measurements were carried out simultaneously to investigate the variation of ultrasonic attributes, particularly the transmitted amplitude. The amplitude variations were linked to the physical processes ongoing during shearing and, hence, the state of contact was qualitatively evaluated according to the amplitude variations. Moreover, different phases were identified before the dynamic failure and the amplitude variations during these phases were studied.

TESTING MATERIAL AND SPECIMEN PREPARATION

Experiments were conducted on layers of granular Ottawa sand (SiO_2). The sand is sourced from the US Silica Company in Ottawa, Illinois. The material is a common standard sand that has been extensively tested and its mechanical properties have been widely studied (Hong and Marone 2005). The purchased sand is commercially known as F75 - Ottawa Sand and has a specific gravity of 2.65. In order to obtain a uniform particle size distribution, the purchased material were sieved according to the ASTM C136 standard. The sand materials used in this study were classified as poorly graded sand, SP, in accordance with descriptions defined by the Unified Soil Classification System (USCS) (ASTM D2488-00), with the mean particle size of 0.58 mm. The particle size distribution curve for the studied materials is shown in Figure 1. The sand was determined to be sub-angular from SEM images using an electron microscope. The SEM images are also shown in Figure 1.

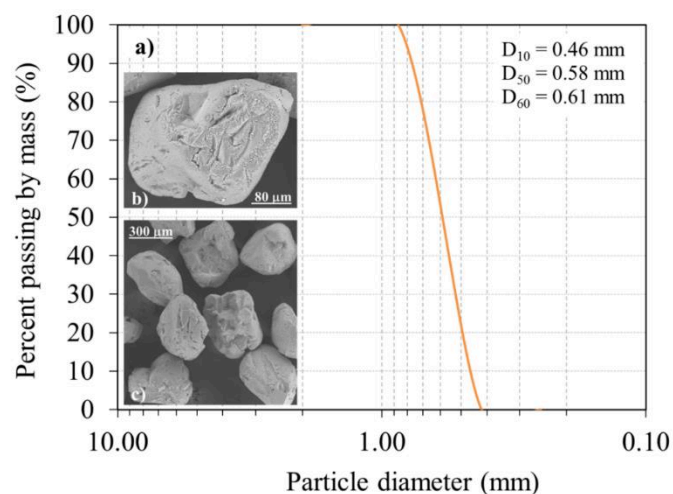


Figure 1. Particle size distribution and SEM images for the Ottawa sand.

Specimens were prepared using oven-dried sand particles mixed with de-aired water to achieve the water content of 10%. This specific water content was selected experimentally to obtain uniform and homogenous specimens with repeatable mechanical and ultrasonic response.

To produce specimen with a uniform moisture content, the moist material was kept in a sealed plastic for 24 h. Thereafter, a 6 mm thick layer was prepared using two 10 cm by 10 cm stainless steel forcing blocks. A leveling lab-jack and four plastic bars were used to control the specimen height and porosity ($n=38\%$).

EXPERIMENTAL SETUP

The schematic view of the direct shear apparatus utilized in this study is shown in Figure 2. The experimental setup incorporates a vertical loading machine, horizontal loading frame, and the ultrasonic system. The horizontal loading frame consisted of three main plates which provide the structure to apply the normal load through a hydraulic flat jack connected to an automated servo controlled hydraulic pump. In this setup, the granular fill layer placed between two grooved stainless steel forcing blocks as well as the transducer holder plates were compressed by the normal load provided by the flat jack. An LVDT was used to measure the changes in layer thickness in real time and throughout the experiment. An automated servo controlled hydraulic loading frame was used to apply shear stress to the specimen. The shear stress and displacement were measured using an internal pressure transducer and three LVDT's placed 120 degrees apart, respectively.

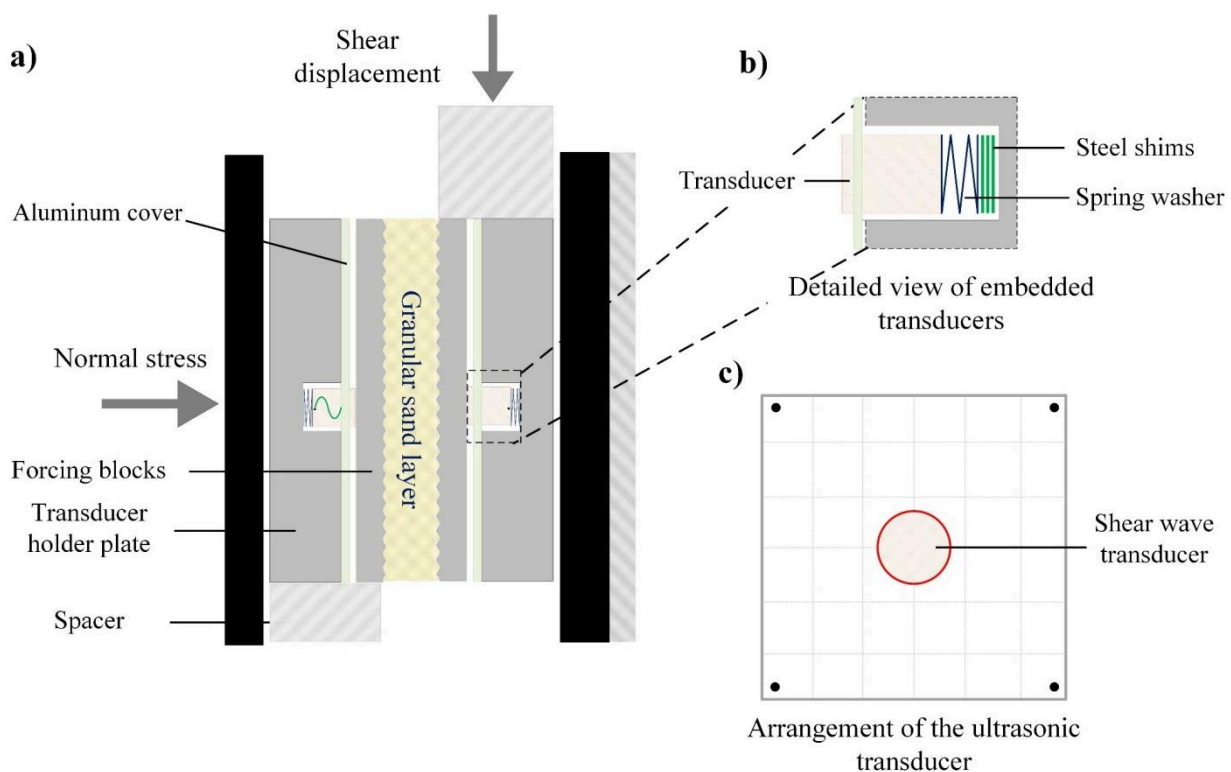


Figure 2. a) Schematic side view of the single direct shear device with embedded ultrasonic transducers; b) Schematic presentation of the details of transducer, spring washer and steel shims embedded in the transducers holder plates; and c) Configuration of the ultrasonic transducers in the transducer holder plate.

This setup is designed to test thin layers of filling materials subjected to compression and shear loads. The granular sand layer was sandwiched between two stainless steel plates. The

forcing blocks were grooved on one side to provide the required friction with the material and were flat on the other side to provide a good contact with the ultrasonic transducers. The stainless steel forcing blocks were able to transfer the normal and shear stresses to the specimen, as well as transferring the ultrasonic waves. The embedded transducers were placed on the two sides of stainless steel plates.

The ultrasonic transducer was embedded into the transducer holder plates and in contact with the forcing blocks. One spring washer and a number of steel shims were placed underneath the transducer to ensure that the contact stress was constant throughout the test by the elastic deformation in spring washers. The spring washer can deform under low values of normal stress, beyond which the washer compresses and the contact stress becomes independent of the applied load. Having a constant contact stress is necessary to ensure high repeatability for the acquired ultrasonic waves (Hedayat 2013). A thin layer of baked honey at 90 degrees C for 90 minutes was used as the coupling material between the surface of the ultrasonic transducer and the forcing block. Honey as a coupling material has produced high repeatable results in previous studies (Hedayat et al. 2014; 2018; Gheibi and Hedayat 2018b).

The ultrasonic transducers used in this study were Olympus V103 with 12.7 mm diameter cylindrical contact transducers, which had a central frequency of 1 MHz. In this study a pulser-receiver (Olympus Panametrics 5077PR) was used to generate signals at a repetition rate of 5 kHz and an amplitude of 300 V.

Fundamental properties of acquired ultrasonic waves, including wave velocity and transmitted peak-to-peak amplitude were examined in this study. The wave velocity was determined according to sample thickness and the wave arrival time. Wave arrival time is defined as the first point where excitation emerges (Inci 2000; Kawaguchi et al. 2001). More details of the methodology used for the determination of wave velocity can be found in Gheibi and Hedayat, (2018b). The maximum transmitted peak-to-peak amplitude was established as the sum of maximum and minimum value for the initial pulse in the received signal, as it is common in ultrasonic wave laboratory studies.

TESTING PROCEDURE

Single direct shear experiments on granular filling material were conducted in this study to investigate the link between frictional mechanisms and ultrasonic attributes under different types of loading. The experiments conducted in this study started with a compression stage, in which the desired level of normal stress was applied first and then kept constant. The shearing phase can be divided into two modes: (a) shearing with a constant displacement rate and (b) shearing under constant shear stress, resulting in creep. The samples were first sheared with a constant displacement rate of 5 $\mu\text{m/s}$ to reach the steady state condition. Thereafter, the creep experiment was conducted, in which the shear stress was reduced to 95% of peak shear strength and was kept constant throughout the test. In this stage, the normal stress was kept constant to stabilize the loading condition on the specimen and minimize the time dependent change in ultrasonic measurements. In order to simulate the condition in rock joints and tectonic faults where effective stress is subjected to reductions due to temperature and hydraulic factors, normal stress was then reduced linearly with time at the rates of 0.0065 and 0.00065 MPa/s to closely observe the sequence of different sliding modes preceding the shear failure (sliding). Experiments were conducted at two different normal stress reduction rates (i.e., 0.0065 and 0.00065 MPa/s) and the normal stress levels were 17.5 and 20 MPa to explore the repeatability of the different frictional mechanisms and their link with the ultrasonic data.

RESULTS AND DISCUSSION

During the compression stage, the normal stress increased linearly with time, and subsequently the thickness of the granular gouge layer gradually decreased. Figure 3 shows the corresponding changes in layer properties with the increase in the normal stress, indicating the change in the amount of effective stress and subsequently the real contact area at the particle scale. This increase in the inter-particle contact area facilitated the transmission of ultrasonic waves with higher energy and therefore the peak-to-peak amplitude for the transmitted amplitude increased (Knuth et al. 2013). The rate of changes in amplitude was not constant and the values increased slightly in the early stage of compression and then increased with a higher rate. Transmitted amplitude is known to be a function of state of contact and the changes in the rate of increase with normal stress shows the occurrence of different mechanisms at different levels of normal stress (e.g. elastic deformation of particles, particles rearrangements and particles comminution) (Kendal and Tabor 1971; Gheibi and Hedayat 2018b). At lower levels of normal stress (less than 8MPa), the particles first experience elastic deformation which results in compression and subtle increase in inter-particle contact area and subsequently transmitted amplitude. However, as the normal stress increases, the force chains experience buckling followed by particles crushing and re-arrangements into a more compact structure. The later mechanisms affect the amount of contact area and evolution in the transmitted amplitude.

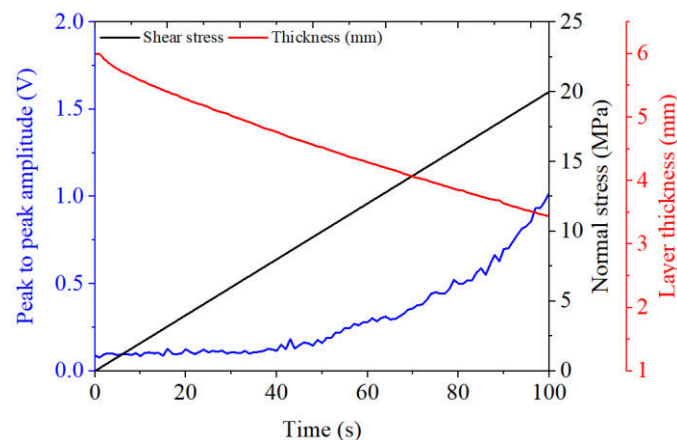


Figure 3. Data showing the compaction and evolution of shear wave amplitude with application of normal stress up to 20 MPa during the initial compression stage.

After the completion of the initial compression stage, the specimens were sheared according to the two steps described in the testing procedure section. Figure 4 shows the evolution of shear stress, shear displacement, normal stress, sliding velocity, peak-to-peak amplitude and wave velocity with time for the two experiments.

Prior to the peak shear strength, the transmitted peak-to-peak amplitude increased significantly in both experiments (See Figure 4, parts c and f). This increase in the peak-to-peak amplitude showed the evolution in the quality of contact points between particles, which could be due to particle rearrangements, compression and comminution (Nagata et al. 2008). Before reaching the steady state condition, amplitude reaches its peak value, showing the maximum amount of densification, which corresponds to the point where the rate of change in layer thickness decreases significantly (Figure 4, parts a and d). Similar to the variation of peak-to-peak amplitude, the wave velocity first increased with the application of shear displacement and

then followed a similar trend as the peak-to-peak amplitude. The general trends in variation of wave velocity were very similar to the peak-to-peak amplitude but the values were less clear than the amplitude, indicating higher reliability of the transmitted amplitude as indicator of grain scale processes occurring during shearing. The layer thickness continuously decreased with the application of shear displacement as observed in similar studies (Samuelson et al. 2009). Specially, for the initial parts of the shear while reaching the steady-state condition, the variations are more pronounced showing the higher rate in layer densification.

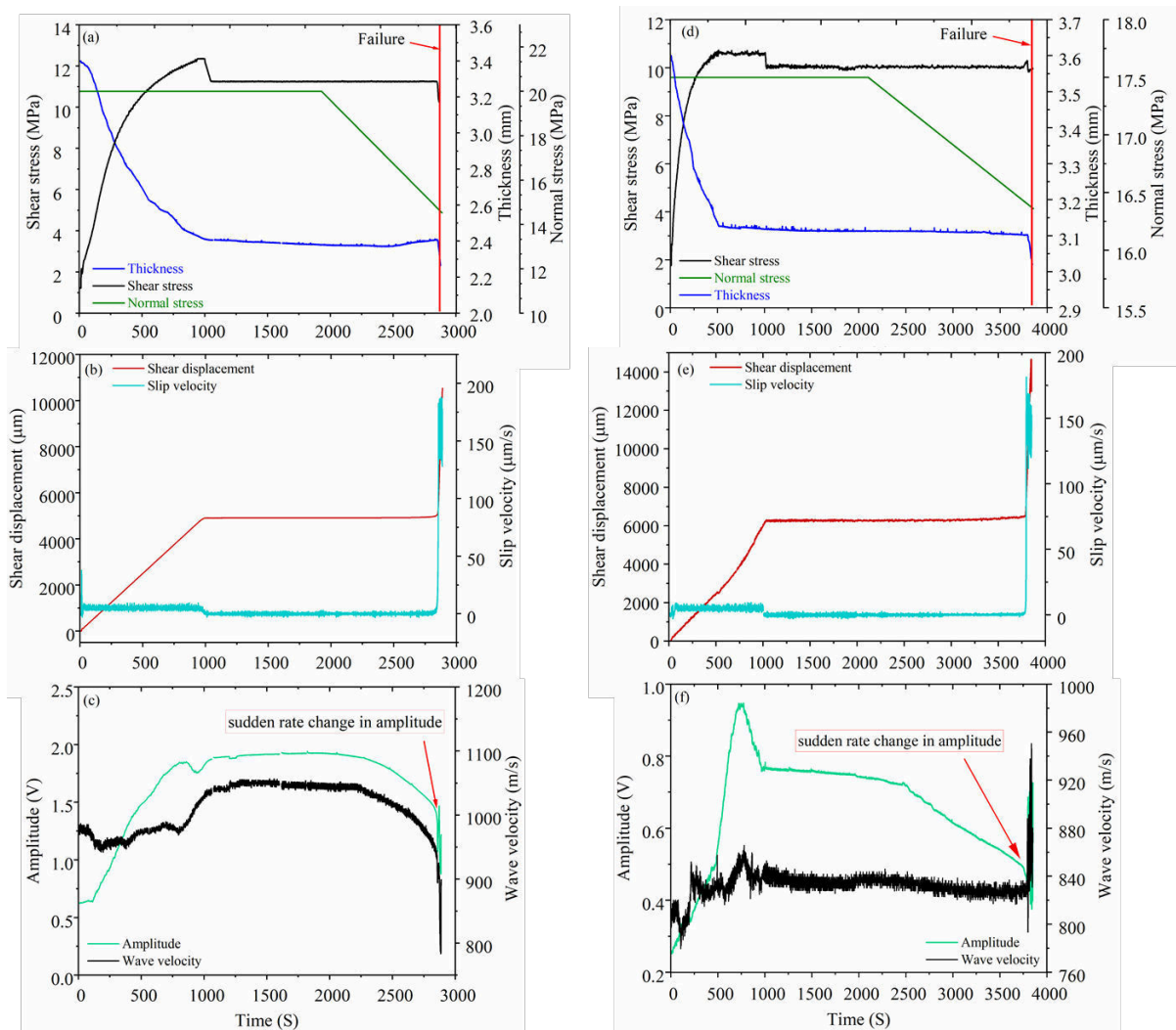


Figure 4. Experimental data during shearing of granular fill layer under 20MPa normal stress (left column) and 17.5 MPa (right column). a, d) Shear stress, layer thickness and normal stress variations. b, e) Changes in shear displacement and slip velocity. c, f) peak to peak amplitude and wave velocity.

With the reduction in shear stress and transition to the stress control mode, the slip velocity reduced significantly, indicating the locking of the granular layer (Figure 4, parts b and e). This phase is considered as the sticking phase, during which the state of contact between particles gradually evolved through micro-scale deformations, creep and healing processes. These processes would favor the ultrasonic waves to travel with higher energy. However, a gradual

decreasing trend was observed in the amplitude values due to the reduction in normal stress despite the fact that the specimens were still locked with negligible shear deformation. The rate of amplitude reduction was almost constant during this phase, while significant changes were observed at a later time with additional reduction of the normal stress and slip initiation (Figure 4, parts c and f). The amplitude variations were followed by significant changes in shear displacement, slip velocity, shear stress and finally the dynamic failure in the granular fill layer.

Figure 5 illustrates the mentioned variations in more details for the experiment conducted under 20 MPa of normal stress. The evolution of different sliding phases prior to the dynamic failure follows a similar trend as the typical three stage creep behavior described by Brantut et al. (2013) for rock joints and Scuderi et al. (2017) for granular materials. According to the variation of slip velocity and as reported in Brantut et al. (2013) and Scuderi et al. (2017), the three phases are shaded with different colors, with the sequence of (1) primary creep, (2) secondary or steady state creep and (3) tertiary creep with dynamic failure. During the primary creep ($t=2786$ to 2835 s), shown as grey color, the slip velocity is very close to zero and the rate of change in amplitude is constant. In the secondary or steady state creep ($t=2835$ to 2847 s), as shaded in green color, the slip velocity starts to increase. This phase could be considered as the slip initiation. During the primary creep phase, the peak-to-peak amplitude decreased with an almost constant rate of -0.002 V/sec (Figure 5). However, during the secondary creep phase, a higher rate of amplitude reduction was observed. During the third phase (shaded in pink), both shear displacement and slip velocity started to increase with higher rates and correspondingly the rate of change in the transmitted amplitude experienced more pronounced variations. The higher rate in amplitude reduction was due to the occurrence of frictional mechanisms in addition to the reduction in the normal stress (e.g., particles movements, force chains rearrangements and contacts breakage). This phase is associated with tertiary creep and dynamic failure and can be further divided into two parts. The first part, 3a, is associated with slip acceleration in which the slip velocity increased at a higher rate and correspondingly the transmitted amplitude decreased with a higher rate. The second part, 3b, is the fast slippage in which the slip velocity reached to its maximum and, correspondingly, amplitude values quickly decreased.

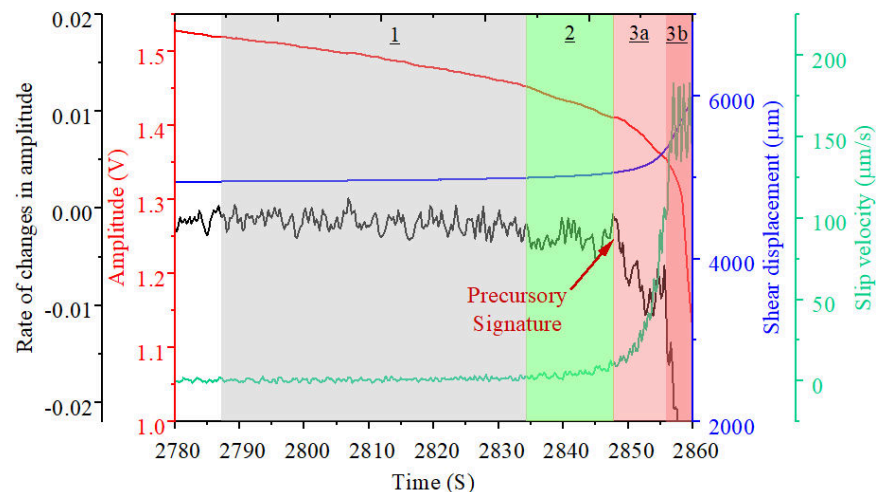


Figure 5. Variation of amplitude, rate of changes in amplitude, shear displacement and slip velocity prior to the dynamic shear failure.

Understanding the link between frictional mechanisms and changes in ultrasonic

measurements under different loading conditions could be informative to evaluate the shear behavior of rock joints and granular materials. Moreover, as explored in recent studies, ultrasonic measurements could be used as an experimental method to detect seismic precursors to the global failure in rock joints and granular materials (Hedayat et al. 2014; Poli 2017). In this study, the point at which the ultrasonic signal amplitude started to decrease at a higher rate (see Figure 5) could be considered as the precursor to the shear failure. In fact, this point is associated with the appearance of weakening mechanisms responsible for slip acceleration and dynamic failure, which took place at low sliding velocities (6 $\mu\text{m/s}$) and about 10 seconds before the fast slippage. Extending and exploring new methodologies for detecting such precursory signatures in laboratory studies and natural settings would enhance the possibilities to predict failure in rock slopes and tectonic fault.

CONCLUSION

In this study, single direct shear experiments were conducted to investigate the impact of normal stress variations on the frictional mechanisms as well as dynamic shear failure in granular fill materials. The granular sand specimens were monitored by ultrasonic shear waves as they were subjected to compressional and shear loads. Shear experiments were conducted in two different displacement and stress control modes. The obtained results showed a close relation between transmitted amplitude and particle scale mechanisms as well as layer thickness variations. It was observed that time dependent mechanisms including creep and healing processes could be captured through the changes in transmitted amplitude. Prior to the dynamic failure, three different phases of creep were identified as well as their impact on the transmitted amplitude. Seismic precursors to dynamic failure were also identified according to the rate of changes in peak-to-peak amplitude.

REFERENCES

- Aragon, L. E., Gheibi, A., Masoumi, H., and Hedayat, A. (2018). "Geophysical Imaging of Frictional Contacts and Processes in Shaly Sandstone Rock Joints." In *52nd US Rock Mechanics/Geomechanics Symposium*. American Rock Mechanics Association.
- Brantut, N., Heap, M. J., Meredith, P. G., and Baud, P. (2013). "Time-dependent cracking and brittle creep in crustal rocks: A review." *J. of Structural Geology*, 52, 17-43.
- Gheibi, A., Slouka, S., and Hedayat, A. (2018). "Ultrasonic investigation of friction processes in granular gouge materials." In *52nd US Rock Mechanics/Geomechanics Symposium*. American Rock Mechanics Association.
- Gheibi, A., and Hedayat, A. (2018a). "The Relation between Static Young's Modulus and Dynamic Bulk Modulus of Granular Materials and the Role of Stress History." In *Proc. 5th Geotechnical and Earthquake Engineering and Soil Dynamics Conf, GEESDV. Austin. TX.* (Vol. 13).
- Gheibi, A., and Hedayat, A. (2018b). "Ultrasonic investigation of granular materials subjected to compression and crushing." *Ultrasonics*, 87, 112-125.
- Hedayat, A., Pyrak-Nolte, L. J., and Bobet, A. (2014). "Precursors to the shear failure of rock discontinuities." *Geophysical Research Letters*, 41(15), 5467-5475.
- Hedayat, A., (2013). "Mechanical and Geophysical Characterization of Damage in Rocks." Ph.D. thesis, Purdue University, West Lafayette, IN.
- Hedayat, A., Haeri, H., Hinton, J., Masoumi, H., and Spagnoli, G. (2018). "Geophysical Signatures of Shear-Induced Damage and Frictional Processes on Rock Joints." *Journal of*

- Geophysical Research: Solid Earth*, 123(2), 1143-1160.
- Hong, T., Marone, C. (2005). "Effects of normal stress perturbations on the frictional properties of simulated faults." *Geochem. Geophys. Geosyst*, 6 (3).
- Inci, G., (2000). "Nondestructive evaluation of compacted clayey soils," *Internal Report, Department of Civil and Environmental Engineering*, Wayne State University, Detroit, Michigan.
- Karakus, M., Liu, Y., Zhang, G., and Tang, H. (2016). "A new shear strength model incorporating influence of infill materials for rock joints." *Geomechanics and Geophysics for Geo-Energy and Geo-Resources*, 2(3), 183-193.
- Kawaguchi, T, Mitachi, T and Shibuya, S (2001). "Evaluation of shear wave travel time in laboratory bender element test." *Proceedings of the 15th. International Conference on Soil mechanics and Geotechnical Engineering (ICSMGE)*, 1: 155-158.
- Kendall, K., and Tabor, D., (1971). "An ultrasonic study of the area of contact between stationary and sliding surfaces. " *In Proceedings of the Royal Society of London A: Mathematical, Physical and Engineering Sciences*, Vol. 323, No. 1554, pp. 321-340, The Royal Society.
- Knuth, M. W., Tobin, H. J., and Marone, C. (2013). "Evolution of ultrasonic velocity and dynamic elastic moduli with shear strain in granular layers." *Granular Matter*, 15(5), 499-515.
- Nagata, K., Nakatani, M., and Yoshida, S. (2008). "Monitoring frictional strength with acoustic wave transmission." *Geophysical Research Letters*, 35(6).
- Naghadehi, M. Z. (2015). "Laboratory study of the shear behaviour of natural rough rock joints infilled by different Soils." *Periodica Polytechnica Civil Engineering*, 59(3), 413-421.
- Poli, Piero. (2017). Creep and slip: "Seismic precursors to the Nuugaatsiaq landslide (Greenland)." *Geophysical Research Letters* 44.17 (2017): 8832-8836.
- Samuelson, J., Elsworth, D., and Marone, C. (2009). "Shear-induced dilatancy of fluid-saturated faults: Experiment and theory." *Journal of Geophysical Research: Solid Earth*, 114(B12).
- Scuderi, M. M., Collettini, C., and Marone, C. (2017). "Frictional stability and earthquake triggering during fluid pressure stimulation of an experimental fault." *Earth and Planetary Science Letters*, 477, 84-96.
- Shrivastava, A. K., and Rao, K. S. (2014). "Effect of infill thickness on shear behaviour of jointed rock under CNS conditions." *Rock Engineering and Rock Mechanics: Structures in and on Rock Masses*, 167.

The Use of the Spectral Element Method for Modeling Stress Wave Propagation in Non-Destructive Testing Applications for Drilled Shafts

Alireza Kordjazi, S.M.ASCE¹; Joseph T. Coe, Ph.D., A.M.ASCE²;
and Michael Afanasiev, Ph.D.³

¹Graduate Research Assistant, Dept. of Civil and Environmental Engineering, Temple Univ., Philadelphia, PA. E-mail: alireza.kordjazi@temple.edu

²Associate Professor, Dept. of Civil and Environmental Engineering, Temple Univ., Philadelphia, PA. E-mail: joseph.coe@temple.edu

³Mondaic Ltd., Zurich, Switzerland. E-mail: michael.afanasiev@mondaic.com

ABSTRACT

The use of stress waves for geophysical and non-destructive testing (NDT) applications continues to grow within the geotechnical community. For example, the quality control and assurance (QC/QA) process for deep foundations often relies on NDT methods such as cross-hole sonic logging (CSL), cross-hole sonic tomography (CST), and parallel seismic (PS) that are based on the propagation of stress waves through the foundation. Although these methods are the standard techniques in the deep foundation industry, they are known to have limitations in detecting defects. Therefore, it becomes important to effectively and efficiently model the propagation of stress waves in order to advance the state of practice with respect to deep foundation NDT. For example, full waveform inversion (FWI) of stress waves is a novel technique that has shown promising performance in providing high resolution images for geophysical/NDT applications at multiple scales of interest. Unlike methods that solely rely on the first time of the arrival of the stress waves, FWI attempts to match entire recorded waveforms. Hence, it requires an accurate simulation of wave propagation through the domain. Moreover, FWI is a computationally expensive approach as it requires multiple iterations to solve the inverse problem. The spectral element method (SEM) offers an efficient solution to the forward problem of wave propagation in terms of both accuracy and computational time. This study first provides a brief overview of the spectral element method. Then the application of SEM in non-destructive testing for quality control and assurance of drilled shafts is presented through a series of numerical simulations that model stress wave propagation for FWI and compare it to a finite-difference method (FDM) approach.

INTRODUCTION

The propagation of stress waves has long been of interest in civil engineering. Seismic wave propagation is sensitive to mechanical and physical properties of the earth materials. This has inspired engineers and geophysicists to develop tools and techniques for subsurface investigations. Such applications include, but are not limited to, site characterizations, seismic site response analysis, and detecting subsurface features such as karst and voids (Park et al. 1999, Hanson et al. 2000; Coe et al. 2016, Rahimi et al. 2018). Non-destructive testing (NDT) techniques based on the propagation of stress waves have also become increasingly popular in geotechnical applications such as quality control and assurance (QC/QA) of the construction of drilled shafts (Brown et al, 2018). Continuous progress in seismic geophysical/NDT technology can be attributed in large part to a better understanding of wave propagation. This can be accomplished through careful field applications and laboratory studies. However, improvements

in the simulation of stress wave propagation play a major role in enhancements to NDT capabilities. For example, there has been a recent increase in the use of the full waveform inversion (FWI) for site characterization (Kallivokas et al. 2013) and NDT (Nguyen and Modrak 2018) in civil and geotechnical engineering applications. FWI is a high-resolution imaging method in which the waveform propagation in the domain under test is iteratively solved. The goal is to find a domain whose synthetic waveforms match properly the acquired waveforms; hence, increasing the importance of simulating wave propagation in complex domains.

There is often no analytical solution to the partial differential equation (PDE) of motion of the stress wave propagation. Numerical techniques are generally used to provide an accurate estimation of the solution to the wave equation (Komatitsch and Tromp 2002; Igel 2016). Numerical methods such as the finite difference method (FDM), however, suffer from limitations in particular when implementing more complex free surface conditions, boundary conditions, and relatively sharp discontinuities in domains. Moreover, the computation time is an important factor for modeling wave propagation in complex domains such as those found in FWI applications. To address some of the limitations of these methods, the spectral element method (SEM) was developed in the 1990's and has since been used extensively in geoscience and geophysical research to simulate the large domains typically encountered in such applications.

This paper provides an account of the main features of the SEM. Through a series of synthetic simulations of deep foundations NDT, forward modeling of stress wave propagation using both SEM and FDM are compared with each other to demonstrate the applicability of SEM at typical geotechnical scales of interest. Finally, the application of the SEM as the solver of a FWI workflow for geotechnical engineering applications is presented.

SPECTRAL ELEMENT METHOD (SEM)

Finite difference method is the most commonly used numerical technique for the simulation of wave propagations (Moczo et al. 2007). However, implementing free surfaces and discontinuous features in FDM are always challenging. For example, some of the schemes for accurate modeling of free surface in FDM require very fine grids that eventually increase the cost of computation. One of the main features of element-based methods such as the finite element method (FEM) is the flexibility in generating complex geometries where meshes can be adapted to the structures (Schuberth 2003). However, FEM has a poor cost-to-accuracy ratio and generally suffers from numerical dispersions due to the use of low-order polynomial approximations (Fichtner 2011). The element size must be reduced to overcome this issue, which can excessively increase computation time.

The pseudo-spectral method address this accuracy issue and provides the benefit of very small amount of numerical dispersion. However, a pseudo-spectral approach poses challenges and difficulties with regard to irregular domains (surfaces) and parallel computations (Fichtner, 2011). The goal of the spectral element method (SEM) is to combine these two methods to take advantage of flexibility of the element-based method (i.e., FEM) and the accuracy of the pseudo-spectral method. SEM with Lagrange polynomial as interpolating basis functions (Komatitsch and Vilotte 1998) allows the development of a diagonal mass matrix, with great advantages for implementation in terms of time scheme and parallelism.

In order to look at the main features that distinguishes the SEM from other numerical methods, a very brief review of the method is presented here. In a one-dimensional (1D) domain the equation of motion can be developed using three force-type terms: